

Disentangling Microbial Syntrophic Mechanisms for Hexavalent Chromium Reduction in Autotrophic Biosystems

Baogang Zhang

China University of Geosciences

Jun Liu (✉ liujun2009sysu@gmail.com)

Sun Yat-Sen University <https://orcid.org/0000-0001-8148-3515>

Yizhi Sheng (✉ shengy5@miamioh.edu)

Miami University

Jiaxin Shi

China University of Geosciences

Hailiang Dong (✉ dongh@cugb.edu.cn)

China University of Geosciences

Research

Keywords: chromium-contaminated groundwater, autotrophic biosystems, genome-resolved metagenomics, methane metabolism, biogeochemical cycles

Posted Date: June 17th, 2020

DOI: <https://doi.org/10.21203/rs.3.rs-35595/v1>

License:  This work is licensed under a Creative Commons Attribution 4.0 International License.

[Read Full License](#)

Version of Record: A version of this preprint was published at Environmental Science & Technology on April 19th, 2021. See the published version at <https://doi.org/10.1021/acs.est.1c00383>.

Abstract

Background: Hexavalent chromium [Cr(VI)] is one of ubiquitous heavy-metal contaminants in groundwater, and electron donors are considered to be a key parameter for Cr(VI) biotransformation. During autotrophic remediation process, however, much remains to be unveiled that how complex syntrophic microbial communities couple Cr(VI) reduction with other elemental cycles.

Results: Two series of Cr(VI)-reducing groundwater bioreactors were independently amended by elemental sulfur (S^0) and iron (Fe^0), and inoculated with the same inoculum. After 160 days incubation, both bioreactors showed the similar archaea-dominating microbiota compositions, whereas a higher Cr(VI) reducing rate and more methane production were detected in the Fe^0 -driven one. Metabolic reconstruction of 23 retrieved genomes revealed complex symbiotic relationships driving distinct elemental cycles coupled with Cr(VI) reduction in bioreactors. In both bioreactors, these inferred Cr(VI) reducers were assumed to live in syntrophy with oxidizers of sulfur, iron, and volatile fatty acids (VFAs) and methane produced by carbon fixers and multi-trophic methanogens, while hydrogen slowly released via an Fe^0 corrosion process might readily facilitate methanogenesis and more methane oxidation might be linked to Cr(VI) reduction in the Fe-bioreactor.

Conclusion: These findings provide insights into mutualistic symbioses of carbon, sulfur, iron and chromium metabolisms in groundwater systems, providing implications for both *in-situ* and *ex-situ* bioremediation of contaminated groundwater.

Background

Chromium (Cr) is a highly toxic heavy metal widely used in industries [1, 2], posing a serious threat to public health and ecological environment, especially groundwater [3, 4]. A recent survey of groundwater contaminants worldwide has revealed a wide distribution of the carcinogenic hexavalent Cr [Cr(VI)] in the form of CrO_4^{2-} and $HCrO_4^-$ [5]. Thus, pathways to efficiently remove excessive Cr(VI) from groundwater have received tremendous attention in the field of environmental science. Microbially-mediated Cr(VI) removal is considered as a promising remediation strategy, which transforms Cr(VI) to less toxic Cr(III) [4, 6–9].

For microbial Cr(VI) reduction, various electron donors (e.g., organic substrates, H_2 , CH_4 , S^0 , and Fe^0) have been utilized, and satisfactory Cr(VI) removal performance has been achieved in these bioreactors treating Cr(VI)-contaminated groundwater [10, 11]. However, addition of organic carbon can induce aquifer pore clogging due to excessive cell growth and increased solubility of Cr(III) as organic-Cr(III) complexes, likely resulting in secondary pollution [11–13]. In addition, potential safety issues from the usage and storage of explosive H_2 and CH_4 gases require precautionary measures before their wide applications in practice [10]. In contrast, S^0 and Fe^0 are advantageous electron donors for both *in-situ* and *ex-situ* remediation of Cr(VI)-contaminated groundwater, due to satisfactory eliminating efficiency, limited secondary pollution, and little safety concern [3, 10, 14]. Furthermore, previous studies have revealed a

number of aerobic and anaerobic microorganisms capable of direct Cr(VI) reduction in nature, such as *Pseudomonas putida* MK1, *Desulfovibrio vulgaris*, *Arthrobacter aurescens*, and *Geobacter sulfurreducens* [7, 15, 16]. These organisms usually harbor soluble and/or membrane-associated Cr(VI) reductases (such as ChrR, Nema, NfsA, cytochromes) [1, 8]. Intriguingly, methanotrophs can not only perform enzymatic Cr(VI) reduction, but also collaborate with other Cr(VI) reducers to indirectly mediate this process [11, 13, 15]. Additionally, recent studies have revealed a vital role of autotrophic microbes in this reduction process, because they can fix inorganic carbon to synthesize organic matter to support heterotrophic Cr(VI) reduction [14, 17]. In brief, the majority of studies regarding Cr(VI) bio-reduction have focused on the kinetics and metabolic potential of some specific microbes [12, 18–20], whereas few attempts have been made to clarify the mechanism of community assembly and functional roles of indigenous microorganisms in Cr(VI)-contaminated natural and artificial groundwater systems.

Laboratory microcosm reactors are an ideal system for distangling the intricate biogeochemical processes as compared to the complex natural ecosystems [21–23]. Our latest research used high-throughput 16S rRNA gene sequencing to illuminate community dynamics in response to the process of Cr(VI) reduction linked to the transformation of S^0 and Fe^0 in autotrophic bioreactors, speculating how those bacteria collaborate to link these geochemical cycles [10, 14]. However, the “real” ecological roles of these inferred participants and their syntrophic relationships remain unclear. What is more, the role of biogas generated during the reduction process is to be unveiled. In the past years, the extensive use of omics approaches (such as genome-resolved metagenomics, single-cell genomics, metatranscriptomics) has made a tremendous contribution to depict metabolic functions of keystone species and the complex and dynamic syntrophic associations in natural microbial communities [24, 25]. To address these gaps, we retrieved draft genomes for core communities in the original inoculum and two series of Cr(VI)-contaminated groundwater bioreactors that were independently amended by S^0 and Fe^0 . Combining with geochemical data, their metabolic pathways were reconstructed to infer syntrophic partnerships. These findings provide new information on metabolic dependencies of microbial syntrophies during Cr(VI) bioreduction, contributing to bioremediation of Cr(VI)-contaminated environments.

Results And Discussion

Bioreactor performance

In this study, two types of electron donors, S^0 and Fe^0 were used for microbially-mediated chromate reduction. Results revealed that the Cr(VI) concentration in both bioreactors decreased significantly and remained stable for each cycle, herein the steady-state biogeochemical process was achieved in these reactors after 160 days incubation (Figure S1). In comparison with the S-bioreactor, the Fe-bioreactor showed a higher reduction rate of Cr(VI) (Fig. 1a). Two peaks corresponding to Cr 2p_{3/2} (576.0-578.0 eV) and Cr 2p_{1/2} (586.0-588.0 eV) in XPS spectrum indicated that the precipitates in both bioreactors were Cr(III) species, typically Cr(OH)₃ (Figure S2a). In the S-bioreactor, a decline of Cr(VI) accompanied an increase of SO_4^{2+} (Fig. 1a), and no sulfite and thiosulfate were detected in the solution, suggesting that

S⁰ oxidation to sulfate may be directly coupled with Cr(VI) reduction. In the Fe-bioreactor, aqueous Fe(II) and Fe(III) were not detected, likely due to the formation of Fe-bearing minerals at circum-neutral pH condition (Figure S2b) [10, 14], suggesting that Cr(VI) reduction may be coupled with Fe⁰ oxidation. The XPS analysis showed these precipitates had two typical peaks assigned to Fe 2p_{1/2} (725.0 – 727 eV) and Fe 2p_{3/2} (710.0 – 712.5 eV) (Figure S2b), which are similar to the peaks of Fe₃O₄ oxides. Interestingly, a time-course increase of methane was measured in the Fe-bioreactor (Fig. 1b), hinting methanogenesis or related methane metabolism in this bioreactor. Besides, CO₂ was detected in both reactors and likely less abundant in the Fe-bioreactor than that in the S-bioreactor within one cycle, and VFAs (e.g., acetate, propionate, isobutyrate, butyrate, isovalerate, and valerate) were produced in both bioreactors (Fig. 1c), revealing that microbial-mediated C metabolism might play vital roles in both systems.

Abiotic experiments without addition of biomass to the bioreactors demonstrated that Cr(VI) reduction was fully attributed to the biotic process in the S-bioreactor, whereas about 14.8 ± 0.7% Cr(VI) was abiotically removed in the first cycle of Fe-bioreactor. After multiple cycles in the Fe-bioreactor, the steady-state removal efficiency remained around 1.9 ± 0.3% of Cr(VI). Therefore, a high reduction efficiency of Cr(VI) in the Fe-bioreactor (98.1 ± 1.2%) was mainly contributed by the biotic process, indicating Fe⁰ passivation inhibit the additional abiotic process. Initial reduction of Cr(VI) in the Fe-bioreactor might be driven by the electrons directly released from Fe⁰ oxidation, producing hydrogen [3, 10]. Although Fe⁰ passivation prevented more abiotic processes, Fe⁰ corrosion could still induce a slow release of hydrogen in Fe-bioreactor [10]. Interestingly, hydrogen concentration was under detection limit in both bioreactors in the final cycle, illustrating that hydrogen may be extensively consumed once released. In brief, distinct geochemical variations in two ‘closed’ ecosystems point to different biogeochemical processes that were occurring.

Microbial community overview

To illuminate the biotic process in both bioreactors, metagenomics was constructed for samples from the original inoculum and bioreactors at the end of Cr(VI) reduction. A total of approximately 104 GB raw data were quality filtered and then co-assembled, yielding 89,774 scaffolds (≥ 500 bp) (Supplementary Table S1). Subsequently, these 9,323 scaffolds (≥ 2000 bp) were binned, generating 23 draft genomes with estimated completeness of 52%-100% and < 1.5% contamination (Supplementary Table S2). These genomes ranged in size from 1.3 to 3.5 Mb with a GC content between 36.25% and 70.86%. Besides, 1,361 to 3,536 putative genes were predicted for individual genomes, with 80 to 97%, 58 to 75% and 75 to 93% of the gene annotation against the NCBI-nr, KEGG, and eggNOG databases, respectively. In addition, we detected 16S rRNA gene sequences in 15 of these 23 retrieved genomes.

The taxonomic classifications of these bins were inferred using a phylogenomic tree based on the concatenated alignment of 16 ribosomal proteins (Fig. 2a). Specifically, these 23 recovered genomes were affiliated with the phyla *Euryarchaeota* (*n* = 7), *Bacteroidetes* (*n* = 4), *Spirochaetes* (*n* = 2), *Actinobacteria* (*n* = 1) and *Candidatus Aminicenantes* (*n* = 1), and the classes *β-Proteobacteria* (*n* = 4), *γ-Proteobacteria* (*n* = 3) and *δ-Proteobacteria* (*n* = 1). The relative abundances of these genomes accounted

for 59%, 73% and 74% of the communities in the original inoculum, and S- and Fe-bioreactors, respectively (Fig. 2b). In the original inoculum, the *Betaproteobacteria* (31.7%), *Gammaproteobacteria* (10.3%), and *Bacteroidetes* (6.4%) were dominant. After 160 days of incubation in S- and Fe-bioreactors, microbial communities were predominated by the *Euryarchaeota* (62.9% and 49.4% in the S- and Fe-bioreactors, respectively), followed by the *Bacteroidetes* (7.6%) in the S-bioreactor, and the *Gammaproteobacteria* (15.0%) and *Spirochaetota* (6.8%) in the Fe-bioreactor (Fig. 2b). Moreover, dominant species changed from *Rhodocyclaceae* QR_Bin.30 (26.1%) and *Xanthomonas* sp. QR_Bin.24 (8.2%) in the original inoculum to *Methanobacterium* sp. QR_Bin.6 (48.8%) and *Bacteroidetes* QR_Bin.18 (5.8%) in the S-bioreactor, and *Methanobacterium* sp. QR_Bin.6 (35.7%), *Gammaproteobacteria* QR_Bin.12 (15.0%), and *Spirochaetes* QR_Bin.15 (6.8%) in the Fe-bioreactor (Fig. 3). These findings indicated a strong selective pressure on microorganisms caused by different substrates, and also implied different mechanisms of microbial-mediated Cr(VI) reduction.

Metabolic potential of key players in bioreactors

Our experimental design capitalized on the niche differentiation required for carbon, nitrogen, sulfur and iron metabolisms coupling with Cr(VI) reduction in the two distinct 'closed' systems. To decipher the potential roles of these microorganisms, their metabolic pathways were reconstructed (Fig. 3).

Sulfur metabolism

The key genes *dsrAB* encoding dissimilatory sulfite reductase, which is considered as the most critical enzyme involved in dissimilatory sulfite reduction and oxidation [26–28], were identified in five recovered genomes (Table S3). The DsrAB phylogenetic tree demonstrated that three betaproteobacterial species (*Thiobacillus* sp. QR_Bin.5 and QR_Bin.21, and *Rhodocyclaceae* QR_Bin.30) possessed the oxidative *dsrAB* genes (Fig. 4a), and the reductive genes were found in *Methanosaeta* sp. QR_Bin.3 and *Spirochaetes* QR_Bin.4. Evidenced by the occurrence of the oxidative *dsrAB*, *dsrEFH*, *aprAB*, and *sat* genes, the three betaproteobacterial species likely carried out sulfur oxidation to sulfate through the reversed dissimilatory sulfate reduction pathway. Besides, they also encoded for sulfide dehydrogenase (*fccAB*), which are essential for sulfide oxidation to sulfur under anoxic conditions [29]. These above results illustrated that the three species enabled complete oxidation from sulfide to sulfate. Furthermore, *Spirochaetes* QR_Bin.4 might oxidize sulfur to sulfite as a part of sulfur disproportionation due to the fact that the reductive *dsrAB* and *dsrD* genes were present in the genome without *dsrEFH* genes [26], and *Rhodocyclaceae* QR_Bin.19 had a potential to mediate the transformation between sulfate and sulfite as it contained *sat* and *aprAB* genes, but they disappeared in both bioreactors. In addition, four betaproteobacterial species (QR_Bin.5, QR_Bin.19, QR_Bin.21 and QR_Bin.30) were capable of converting thiosulfate to sulfate due to the identified SOX system and poly-S (sulfide_{n-1}) transformation (*sqr* and *hyd*), which accounted for 31.7% and 2.5% in the original inoculum and S-bioreactor, respectively. The above findings indicated an underlying synergetic and collaborative relationship for these microorganisms to complete the sulfur cycle.

Iron metabolism

Iron is not only a micronutrient for nearly all life on Earth, but also serves as an electron donor or acceptor by iron-oxidizing/reducing microorganisms [30, 31]. This study revealed that *Gammaproteobacteria* QR_Bin.7, *Candidatus Aminicenantes* QR_Bin.23 and *Bacteroidetes* QR_Bin.26 were able to encode the cluster 3-affiliated Cyc2 homologs (Supplementary Table S2), which have been biochemically characterized to catalyze iron oxidation in *Acidithiobacillus ferrooxidans* [32] and are also found in neutrophilic, obligate iron-oxidizers [33], suggesting that they were potential iron-oxidizers. Moreover, *Thiobacillus* sp. QR_Bin.5 was inferred to carry out the potential for iron reduction/oxidation owing to the detection of *mtoA* and *mtrB* genes and the absence of the *mtrC* gene [34]. Previous studies have demonstrated that MtoA is homologous to the iron-reducing enzyme, MtrA, of *Shewanella oneidensis* MR-1, and in fact, it has been evidenced to rescue Δ mtrA mutants of MR-1, partially recovering the ability to reduce ferric iron [35]. Despite this, the MtoA homologs are frequently encoded by known and suspected iron-oxidizing bacteria [34], and the MtrC homolog, an outer-membrane cytochrome thought to participate in dissimilatory iron reduction [36], was missing in this species. Thus, we can not rule out the possibility that this species may use this enzyme to oxidize iron as previously proposed [35].

Methane metabolism

An interesting phenomenon attracted attention that methanogenesis was observed in the Fe-bioreactor with no methane detected in the S-bioreactor (Fig. 1b), despite the community compositions in the two bioreactors were highly similar (Fig. 2b). The key *mcrABG* genes encoding the methyl-coenzyme M reductase (MCR) complex were identified in all archaeal bins (Supplementary Table S3), suggesting that these archaea enriched in bioreactors were the important actors in methane metabolism. To unravel evolutionary relationships and characteristics of these MCR complexes detected, we built a phylogenetic tree using the concatenated alignment of McrABG subunits (Fig. 4b). Results revealed that these archaea could code for canonical MCR complexes, as they formed clusters with previously studied methanogens such as *Methanomicrobiales*, *Methanobacteriales*, and *Methanomassiliicoccales* [37]. Even so, we cannot rule out the possibility that they may use this enzyme for anaerobic oxidation of methane (AOM) as previously reported [38, 39]. The above-mentioned difference might be due to that in the Fe-bioreactor, H_2 abiotically produced by Fe^0 facilitated hydrogen-dependent methanogenesis [3, 10], resulting in a high CH_4 concentration in the headspace of this reactor. However, for the S-bioreactor, a trace amount of methane generated by methanogens might be rapidly oxidized by methanotrophs, when coupled to sulfate or metal reduction by themselves or other bacteria [37, 40–42].

According to the substrate use, methanogens are broadly characterized as hydrogenotrophic (H_2 and CO_2), acetoclastic (acetate), methylotrophic ($X-CH_3$) and H_2 -dependent methylotrophic (H_2 and $X-CH_3$) [37, 39]. Thus, *Methanolinea* sp. QR_Bin.1 and QR_Bin.22, and *Methanobacterium* sp. QR_Bin.6, QR_Bin.11 and QR_Bin.13 were inferred to be putative hydrogenotrophic methanogens, resulting from the identification of *m-WL*, *mtrABCDEFGH*, *mcrABG*, and *frhA/ehbN* genes (encoding the [Ni-Fe] hydrogenase) as previously reported [38, 39]. Remarkably, *Methanobacterium* sp. QR_Bin.6 and QR_Bin.11, and

Methanolinea sp. QR_Bin.22 also coded for the carbon monoxide dehydrogenase-acetyl-CoA synthase (Codh-Acs) complex. This complex could activate acetate to generate reduced ferredoxin and methyl- H_4 MPT, a marker enzyme for acetoclastic methanogenesis, illustrating that these bins had a potential to perform both hydrogenotrophic and acetoclastic methanogenesis. The result was inconsistent with previous findings of the close lineages *Methanobacterium formicicum*, *Methanolinea* sp. SDB and *Methanolinea tarda* sp. NOBI-1 that are considered to be hydrogenotrophic methanogens [37]. Besides, *Methanosaeta* sp. QR_Bin.3 was also inferred to carry out acetoclastic methanogenesis, as members of the genus *Methanosaeta* are specialized on acetate degradation [37]. Moreover, *Methanomassiliicoccus* sp. QR_Bin.16 had the potential for H_2 -dependent methylotrophic methanogenesis, evidenced by the fact that this species could code for methyltransferases to support methyl-dependent methanogenesis from methanol (*mtaABC*), methanethiol (*mtsAB*) and methylamines (*mtmB*, *mtbB* and *mtbC*, and *mttB* and *mttC*), and previous studies showed that *Methanomassiliicoccus* populations were H_2 -dependent methylotrophic methanogens [37, 43].

Apart from the anaerobic methanogens, we found that *Gammaproteobacteria* QR_Bin.12 was a putative methane-oxidizing bacteria (MOB) due to the presence of the key genes *pomABC* encoding methane monooxygenase. This bin accounted for 15.0% of relative abundance in the Fe-bioreactor but only 0.65% in the S-related one. Previous studies revealed methane monooxygenases in a small number of bacterial species affiliated with the *Gamma*- and *Alpha*-*proteobacteria* and *Verrucomicrobia* habitating the aerobic-anaerobic interface [44–46], and that these microorganisms could use a variety of terminal electron acceptors (e.g., oxygen, nitrate) for methane oxidation [47–49]. As such, the methane produced by methanogens might be partially oxidized by *Gammaproteobacteria* QR_Bin.12, particularly in the Fe-bioreactor.

Chromium reduction

The primary purpose of this study was to investigate how Cr(VI) reduction was coupled with other biogeochemical cycles, thus genes involved in Cr(VI) reduction were confirmed in these retrieved genomes (Supplementary Table S3). *Methanolinea* sp. QR_Bin.1 harbored the potential to encode NfsA, an oxygen-insensitive nitroreductase and also a flavoprotein that can reduce Cr(VI) to less soluble and toxic Cr(III) [8, 50], implying that it was a putative chromate reducer. Notably, this reductive process would produce intracellular reactive oxygen species (ROS) that combine with DNA-protein complexes to cause cell DNA and protein damage [50, 51]. Besides that, the *nemaA* gene was identified in *Spirochaetes* QR_Bin.4, *Thiobacillus* sp. QR_Bin.5 and QR_Bin.21, *Gammaproteobacteria* QR_Bin.7 and QR_Bin.12, and *Rhodocyclaceae* QR_Bin.30. The FMN-dependent NADH-azoreductase gene *azoR* was found in *Rhodocyclaceae* Bin.19 and *Thiobacillus* sp. QR_Bin.21. The identification of these genes, which was confirmed to be involved in chromate reduction [8], suggests that all these microorganisms were potential chromate reducers. Previous research have proven that the nethylmaleimide reductase (NemaA) belonging to the old yellow enzyme family of flavoproteins could use one or two electrons from the cofactors to reduce chromate intracellularly [52].

Under many oxygen-depleted conditions, Cr(VI) can be reduced extracellularly by coupling with intracellular oxidation of electron donors such as carbohydrates, proteins, fats, and hydrogen [2, 7, 8]. The cytochrome c3 was identified in most of these recovered genomes in both bioreactors (Supplementary Table S3), suggesting that they were able to reduce Cr(VI) through the electron transfer chain. The cytochrome families are frequently shown to participate in extracellular Cr(VI) reduction under anaerobic conditions, including cytochrome c3 of *Desulfovibrio vulgaris* [53] and *Desulfomicrobium norvegicum* [54, 55]. Furthermore, the reduction of Cr(VI) may also take place by chemical reactions associated with organic compounds present in intra/extra cellular, such as amino acids, nucleotides, sugars, vitamins, organic acids and glutathione [2, 7, 8]. In addition to the enzymatic reduction, chromate efflux from cells is an efficient and widespread mechanism to decrease chromium toxicity [56, 57]. The protein ChrA, a hydrophobic membrane protein that can export chromate from cytoplasm or periplasm driven by the proton motive force [8, 58], was inferred to be encoded in *Conexibacter* sp. QR_Bin.2, *Thiobacillus* sp. QR_Bin.5 and QR_Bin.21, *Gammaproteobacteria* QR_Bin.7, and *Spirochaetes* QR_Bin.15. In brief, mechanisms of microbial-mediated Cr(VI) reduction are extremely complicated with multiple possible pathways and unstable redox intermediates [4, 6–9].

Carbon fixation

After one day incubation, relatively stable CO₂ concentrations were observed in both bioreactors (Fig. 1b), thus carbon fixation might exist. Among these potential autotrophs (including four archaea and three bacteria), only *Methanobacterium* sp. QR_Bin.11 might use the Wood-Ljungdahl (WL) pathway to fix CO₂, and the others likely perform the Calvin-Benson-Bassham (CBB) cycle (Fig. 3 and Table S3). Intriguingly, these putative archaeal autotrophs and one potential bacterial autotroph (*Methanolinea* sp. QR_Bin.1 and QR_Bin.22, *Methanosaeta* sp. QR_Bin.3, *Methanobacterium* sp. QR_Bin.11, *Methanomassiliicoccus* sp. QR_Bin.16 and *Thiobacillus* sp. QR_Bin.21) were enriched in both bioreactors relative to the original inoculum (Fig. 3), revealing that *Bacteria* primarily contributed to carbon fixation in the original inoculum, whereas *Archaea* became the main carbon fixers after a long-term incubation in both bioreactors.

Nitrogen metabolism

Key genes relevant to dissimilarity nitrate reduction were evaluated (Supplementary Table S3), and the results revealed that ten species were likely involved in the process transforming nitrate to ammonia, of which *Thiobacillus* sp. QR_Bin.21 and *Gammaproteobacteria* QR_Bin.12 were the main participants in the S- and Fe-bioreactors, respectively. The pentaheme nitrite reductase (*nrfAH*), essential for respiratory nitrite ammonification, was identified in *Spirochaetes* QR_Bin.4, suggesting that it might be responsible for nitrite reduction to ammonia. Interestingly, the *nifDKH* genes encoding nitrogenase for nitrogen fixation were confirmed in *Euryarchaeota*, including *Methanosaeta* sp. QR_Bin.3, *Methanobacterium* sp. QR_Bin.6 and QR_Bin.11, and *Methanolinea* sp. QR_Bin.22, illustrating that these archaea were potentially responsible for supplying organic nitrogen for cell growth in the bioreactors.

Fermentation

The detection of VFAs in both bioreactors gave evidence for microbial fermentation [59] (Fig. 1c). The present study showed that most of the recovered species were able to produce acetate via the Pta-Ack pathway (the *pta-ackA* genes) and acylphosphatase (*acyP*) and/or perform ethanol fermentation due to the identification of *adh* gene in both bioreactors rather than in the original inoculum. In contrast, only *Bacteroidetes* QR_Bin.27 harbored the potential to produce lactate due to the *LDH* gene identified.

VFA oxidation

The generated VFAs, e.g., acetate, butyrate, propionate (Fig. 1c), could be oxidized by heterotrophic microorganisms via the reversed WL pathway [60], beta-oxidation pathway [61, 62], or methylmalonyl-CoA pathway [63], linking to the reduction of sulfate, ferric iron and chromium to generate energy for cells [64–66]. As only *Methanobacterium* sp. QR_Bin.11 harbored key genes encoding the WL pathway [67], this species might oxidize acetate via the reversed WL pathway when CO₂ was depleted. The complete beta-oxidation pathway were found in *Spirochaetes* QR_Bin.4 and gammaproteobacterium QR_Bin.12 (Supplementary Table S3), unveiling their underlying potentials to catalyze butyrate [62]. The complete conventional propionate oxidation pathway, methylmalonyl-CoA pathway [63], were detected in *Conexibacter* sp. QR_Bin.2, *Candidatus Aminicenantes* QR_Bin.23, and *Bacteroidetes* QR_Bin.18 and QR_Bin.26, of which *Bacteroidetes* QR_Bin.18 and QR_Bin.26 potentially mediated the conversion of propionate to succinate and then to acetate in bioreactors. Accordingly, these VFA-oxidizing microorganisms may play an imperative role in the transformation of Cr(VI) to Cr(III) in bioreactors, analogous to previous findings [10, 14]. In addition, the oxidation of butyrate and propionate produces the methanogenic precursors such as acetate [62, 63], which can further facilitate acetoclastic methanogenesis [37].

Integrating inferred niches and activities in bioreactors

In the two bioreactors, despite different substrates (S⁰ and Fe⁰) were used, a highly similar community composition appeared to be involved in efficient Cr(VI) removal (Fig. 2). Distinct biogeochemical processes suggest that not only methanogens but also methanotrophs were involved. Moreover, diverse syntrophic metabolisms were found between Cr(VI) reduction and the oxidation of methane, sulfur, iron and acetate in the two 'closed' bioreactors (Fig. 5), indicating a metabolic mutualism among different functional members.

In the S-bioreactor, Cr(VI) reduction may be coupled with three pathways, AOM by anaerobic methane-oxidizing archaea (ANME), VFAs oxidation by VFA-oxidizers, and sulfur oxidation by sulfur-oxidizers. First, methane was likely produced via hydrogenotrophic, acetoclastic and H₂-dependent methylotrophic methanogenesis. Nonetheless, as methane flux was below the limit of detection in this bioreactor, the generated methane may be oxidized immediately by ANME and methane-oxidizing bacteria (MOB) that possibly cooperated with sulfate- and metal-reducing bacteria [37, 40–42]. The *mcr* genes do not merely encode the key enzyme, MCR complexes for methanogenesis, but are also present in ANME to reversely oxidize methane, and the [Ni-Fe] hydrogenases (e.g., VhoA, MvhA, FrhA, and EhbN) are an additional indicator for methane-oxidizing potential [37–39]. In this study, two enriched archaea (*Methanosaeta* sp.

QR_Bin.3 and *Methanomassiliicoccus* sp. QR_Bin.16) did not code for the [Ni-Fe] hydrogenases, but harbored key genes for dissimilarity sulfate reduction (DsrAB) or Cr(VI) reduction (cytochrome c3), thereby they *per se* possibly hold the potential to couple AOM with the reduction of SO_4^{2-} or Cr(VI). Next, under elevated CO_2 in the S-bioreactor, the putative autotrophic *Methanosaeta* sp. QR_Bin.11, *Methanolinea* sp. QR_Bin.22 and *Thiobacillus* sp. QR_Bin.21 could fix inorganic carbon to support chemolithoautotrophic growth under anaerobic conditions. The resulting dissolved organic carbon (DOC) would be used to ferment into acetate, lactate, methanol or other VFAs by *Bacteroidetes* QR_Bin.18 and QR_Bin.27 that might be further utilized to produce methane or oxidized by heterotrophic *Bacteroidetes* QR_Bin.26 when coupled with Cr(VI) reduction. Lastly, S^0 could be directly used as an effective reductant for Cr(VI) reduction by sulfur-oxidizer *Thiobacillus* sp. QR_Bin.21, which coupled sulfur oxidation with Cr(VI) reduction.

In the Fe-bioreactor, the reduction of Cr(VI) could be coupled with methane oxidation by MOB and organic matter oxidation by acetate-oxidizing heterotrophs. Prior studies have demonstrated that Fe^0 is readily utilized as a slow-release electron donor for methanogenesis [68]. The electron transfer mechanism from Fe^0 to microorganisms is through H_2 , which is generated by the chemical reaction of Fe^0 with H_2O under anaerobic conditions. In consideration of the lower CO_2 and higher acetate (Figs. 1b and 1c), the generated H_2 tended to explain the obviously higher CH_4 production in Fe-bioreactor than that in S-bioreactor (Fig. 1b), despite both reactors harbored the similar archaea-dominating communities where the hydrogen-dependent methanogenesis dominated. A putative MOB gammaproteobacterium QR_Bin.12, which harbored both *pomABC* and *nemaA*, constituted the highest abundance in the Fe-bioreactor, primarily owing to the sufficient methane as electron donor. Inconsistent to ANME-mediated AOM in the S-bioreactor, this MOB would perform AOM coupled with Cr(VI) reduction in this bioreactor, which was possibly one of the major contributors for Cr(VI) reduction and might partly explain the higher reduction rate in the Fe-bioreactor (Fig. 1b). Similar to the S-bioreactor, VFA-oxidizing heterotroph *Bacteroidetes* QR_Bin.26 and gammaproteobacterium QR_Bin.12 could also catalyze Cr(VI) reduction in the Fe-bioreactor, and the produced acetate via VFA oxidation can support methanogenesis. Although the bioreactor was running under a steady-state condition and low abiotic Fe(II) oxidation (< 2%) was detected, we could not rule out that the generated Fe(II) may abiotically reduce Cr(VI) due to its strong reducing potential [10, 14].

Conclusions

Herein, genome-resolved metagenomics was informative to elucidate the potential geochemical roles of individual microbial species in S^0 - and Fe^0 -bioreactors for Cr(VI) removal from groundwater. Multiple syntrophic interactions among these keystone members were inferred to couple Cr(VI) reduction with the oxidation of sulfur, iron, VFAs and methane in these autotrophic 'closed' systems. These novel microbial insights advance our knowledge regarding mechanisms involved in Cr(VI) reduction, and guide the development of bioremediation strategies of those Cr(VI)-contaminated environments. Nonetheless,

precise mechanisms governing syntrophic pathways for microbial Cr(VI) reduction remain to be elucidated through a combined isotopic and 'omics' strategy.

Materials And Methods

Reactor setup, operation and chemical analysis

Two series of experimental settings were performed that each setting had a biotic (inoculated with anaerobic inoculum) and an abiotic (none-inoculated) bioreactor. Each setting was amended with 5 g S⁰ or Fe⁰ as potential electron donors for Cr(VI) reduction. A previously described 200 mL synthetic groundwater was used as a medium [10, 14], containing 0.504 g NaHCO₃, 0.2464 g CaCl₂, 0.035 g NH₄Cl, 1.0572 g MaCl₂·6H₂O, 0.4459 g NaCl, 0.0283 g KCl, and 0.029 g KH₂PO₄. K₂CrO₄ was periodically dosed to the reactors as a source of Cr(VI). All experiments were conducted in an anaerobic chamber to avoid S⁰ or Fe⁰ oxidation by oxygen at room temperature (22 ± 2 °C). Long-term incubation was conducted in all bioreactors by feeding synthetic groundwater with Cr(VI) at multiple cycles (each for 120 h), and replenishing the medium until achieving a steady-state condition in ~ 160 days. After that, a new cycle was conducted, and time-source supernatants in both S- and Fe-bioreactors were collected to determine microbial metabolites. Abiotic reactors without inoculation serve as controls under identical conditions. The pH, concentration of Cr(VI), total dissolved Cr, Fe(II), total dissolved Fe, sulfate, sulfite, and thiosulfate were measured according to the previously described methods [10]. Gas chromatograph (Agilent 4890, J&W Scientific, Folsom, CA) equipped with a flame ionization detector was used to identify the potential reaction intermediates (volatile fatty acids, VFAs) and gas (CH₄, CO₂, H₂) produced in the headspace of the bioreactors. The Cr or Fe species in solid precipitates in the two bioreactors were characterized by X-ray photoelectron spectroscopy (XPS) (XSAM-800, Kratos, UK).

Community DNA extraction and sequencing

Samples (0.5 g per sample) were collected from the original inoculum, and S- and Fe-bioreactors at the end of the final cycle, respectively. Community DNA was extracted using FastDNA SPIN Kit for Soil (Qiagen, Valencia, CA). Subsequently, these high-quality DNA samples were sent to the Majorbio Company (Shanghai, China) to construct Illumina libraries with an insert size of 300 bp, and then were sequenced on an Illumina HiSeq 4000 platform in PE150 mode.

Genome-resolved metagenomic analysis

Raw sequencing reads were deduplicated and quality-trimmed using Sickle (version 1.33) with the parameters “-q 20 -l 50”, as described in our previous studies [27]. All high-quality datasets were co-assembled using SPAdes (version 3.11.0) with the parameters “-k 21,33,55,77,99 -meta” [27]. To calculate the scaffold coverage, all high-quality reads from each dataset were mapped to these assembled scaffolds (≥ 2000 bp) using BMap with the parameters “minid = 0.97, local = t”. Then these scaffolds were divided into genomic bins based on their tetranucleotide frequencies and coverages using MetaBAT (version 0.32.4) with the parameters “-m 2000 -unbinned” [69]. These retrieved genomes were evaluated

for genome completeness, potential contamination and strain heterogeneity using CheckM [70]. The genomic bins were further optimized to obtain high-quality genomes as previously reported [71].

A total of 23 genomes with $\geq 50\%$ completeness and $\leq 5\%$ contamination were submitted to the JGI IMG/MER system for gene calling and annotation [72]. Meanwhile, the gene annotation was manually curated and revised by searching genes against the NCBI-nr, KEGG, eggNOG, and Pfam databases. The genes for Fe metabolism were annotated by FeGenie [34]. These genomes were taxonomically assigned based on the Genome Taxonomy Database using GTDB-Tk (version 0.1.3) [70]. Ribosomal protein S3 (rpS3) was used as a phylogenetic marker for relative abundance analysis [71]. All rpS3 were identified using AMPHORA2 [73], and their coverages were determined based on the coverages of the corresponding scaffolds. The relative abundance of each bin was calculated by dividing the coverage of its rpS3 by the total coverage of all rpS3 in the community.

Phylogenomic and phylogenetic analyses

The 22 retrieved genomes and 288 reference genomes available in the Genome Taxonomy Database were applied to construct a phylogenomic tree based on a concatenated alignment of 16 ribosomal proteins as previously suggested [27, 74]. In brief, each of the 16 ribosomal protein sequences was aligned using MAFFT (version 7.3.13) [75], and then trimmed using TrimAL with the parameters “-gt 0.95 -cons 50” [76]. The curated alignments were concatenated, and a phylogenomic tree was built using IQ-TREE (version 1.6.10) with the parameters “LG + I + G4 -alrt 1000 -bb 1000” [77]. Besides, phylogenetic analyses were performed for the *dsrAB* and *mcrABG* genes as mentioned above. The generated treefiles were uploaded to iTOL for visualization and formatting.

Declarations

Ethics approval and consent to participate

Not applicable

Consent for publication

Not applicable

Availability of data and materials

The sequencing data is submitted to sequence read archive (SRA, <https://www.ncbi.nlm.nih.gov/sra>). Please contact author for data requests.

Competing interests

The authors declare that they have no competing interests

Funding

This research work was supported by the National Natural Science Foundation of China (NSFC) (No. 41672237, 41702262, and 41630103) and the Beijing Natural Science Foundation (No. 8192040).

Authors' contributions

BZ designed and supervised experiments, and revised the manuscript. JL and YS analysed metagenomic data, drafted the manuscript, and revised the manuscript. JS monitored bioreactor performance and prepared DNA for sequencing. HD supervised and revised the manuscript. All authors read and approved the final manuscript.

Acknowledgements

Not applicable

References

1. Dhal B, Thatoi HN, Das NN, Pandey BD: **Chemical and microbial remediation of hexavalent chromium from contaminated soil and mining/metallurgical solid waste: A review.** *Journal of Hazardous Materials* 2013, **250**:272-291.
2. Shahid M, Shamshad S, Rafiq M, Khalid S, Bibi I, Niazi NK, Dumat C, Rashid MI: **Chromium speciation, bioavailability, uptake, toxicity and detoxification in soil-plant system: A review.** *Chemosphere* 2017, **178**:513-533.
3. Puls RW, Paul CJ, Powell RM: **The application of in situ permeable reactive (zero-valent iron) barrier technology for the remediation of chromate-contaminated groundwater: a field test.** *Applied Geochemistry* 1999, **14**:989-1000.
4. Fruchter J: **In situ treatment of chromium-contaminated groundwater.** *Environmental Science & Technology* 2002, **36**:464A-472A.
5. Hausladen DM, Alexander-Ozinskas A, McClain C, Fendorf S: **Hexavalent Chromium Sources and Distribution in California Groundwater.** *Environmental science & technology* 2018, **52**:8242-8251.
6. Fernandez PM, Vinarta SC, Bernal AR, Cruz EL, Figueroa LIC: **Bioremediation strategies for chromium removal: Current research, scale-up approach and future perspectives.** *Chemosphere* 2018, **208**:139-148.
7. Cheung KH, Gu JD: **Mechanism of hexavalent chromium detoxification by microorganisms and bioremediation application potential: A review.** *International Biodeterioration & Biodegradation* 2007,

59:8-15.

8. Thatoi H, Das S, Mishra J, Rath BP, Das N: **Bacterial chromate reductase, a potential enzyme for bioremediation of hexavalent chromium: A review.** *Journal of Environmental Management* 2014, **146**:383-399.
9. Pradhan D, Sukla LB, Sawyer M, Rahman P: **Recent bioreduction of hexavalent chromium in wastewater treatment: A review.** *Journal of Industrial and Engineering Chemistry* 2017, **55**:1-20.
10. Shi JX, Zhang BG, Qiu R, Lai CY, Jiang YF, He C, Guo JH: **Microbial Chromate Reduction Coupled to Anaerobic Oxidation of Elemental Sulfur or Zerovalent Iron.** *Environmental Science & Technology* 2019, **53**:3198-3207.
11. Luo JH, Wu MX, Liu JY, Qian GR, Yuan ZG, Guo JH: **Microbial chromate reduction coupled with anaerobic oxidation of methane in a membrane biofilm reactor.** *Environment International* 2019, **130**.
12. Lai CY, Zhong L, Zhang Y, Chen JX, Wen LL, Shi LD, Sun YP, Ma F, Rittmann BE, Zhou C, et al: **Bioreduction of Chromate in a Methane-Based Membrane Biofilm Reactor.** *Environmental Science & Technology* 2016, **50**:5832-5839.
13. Lu YZ, Chen GJ, Bai YN, Fu L, Qin LP, Zeng RJX: **Chromium isotope fractionation during Cr(VI) reduction in a methane-based hollow-fiber membrane biofilm reactor.** *Water Research* 2018, **130**:263-270.
14. Zhang BG, Wang ZL, Shi JX, Dong HL: **Sulfur-based mixotrophic bio-reduction for efficient removal of chromium (VI) in groundwater.** *Geochimica Et Cosmochimica Acta* 2020, **268**:296-309.
15. Al Hasin A, Gurman SJ, Murphy LM, Perry A, Smith TJ, Gardiner PHE: **Remediation of Chromium(VI) by a Methane-Oxidizing Bacterium.** *Environmental Science & Technology* 2010, **44**:400-405.
16. Horton RN, Apel WA, Thompson VS, Sheridan PP: **Low temperature reduction of hexavalent chromium by a microbial enrichment consortium and a novel strain of *Arthrobacter aurescens*.** *Bmc Microbiology* 2006, **6**.
17. Shi C, Cui Y, Lu J, Zhang B: **Sulfur-based autotrophic biosystem for efficient vanadium (V) and chromium (VI) reductions in groundwater.** *Chemical Engineering Journal* 2020, **395**:124972.
18. Chung J, Nerenberg R, Rittmann BE: **Bio-reduction of soluble chromate using a hydrogen-based membrane biofilm reactor.** *Water Research* 2006, **40**:1634-1642.
19. Belchik SM, Kennedy DW, Dohnalkova AC, Wang YM, Sevinc PC, Wu H, Lin YH, Lu HP, Fredrickson JK, Shi L: **Extracellular Reduction of Hexavalent Chromium by Cytochromes MtrC and OmcA of *Shewanella oneidensis* MR-1.** *Applied and Environmental Microbiology* 2011, **77**:4035-4041.
20. Chirwa EMN, Wang YT: **Hexavalent chromium reduction by *Bacillus* sp. in a packed-bed bioreactor.** *Environmental Science & Technology* 1997, **31**:1446-1451.
21. Speth DR, in 't Zandt MH, Guerrero-Cruz S, Dutilh BE, Jetten MSM: **Genome-based microbial ecology of anammox granules in a full-scale wastewater treatment system.** *Nature Communications* 2016, **7**.
22. Cai C, Leu AO, Xie GJ, Guo JH, Feng YX, Zhao JX, Tyson GW, Yuan ZG, Hu SH: **A methanotrophic archaeon couples anaerobic oxidation of methane to Fe(III) reduction.** *Isme Journal* 2018, **12**:1929-

1939.

23. Nobu MK, Narihiro T, Rinke C, Kamagata Y, Tringe SG, Woyke T, Liu WT: **Microbial dark matter ecogenomics reveals complex synergistic networks in a methanogenic bioreactor.** *Isme Journal* 2015, **9**:1710-1722.
24. Bertin PN, Heinrich-Salmeron A, Pelletier E, Goulhen-Chollet F, Arsene-Ploetze F, Gallien S, Lauga B, Casiot C, Calteau A, Vallenet D, et al: **Metabolic diversity among main microorganisms inside an arsenic-rich ecosystem revealed by meta- and proteo-genomics.** *Isme Journal* 2011, **5**:1735-1747.
25. Pernthaler A, Dekas AE, Brown CT, Goffredi SK, Embaye T, Orphan VJ: **Diverse syntrophic partnerships from-deep-sea methane vents revealed by direct cell capture and metagenomics.** *Proceedings of the National Academy of Sciences of the United States of America* 2008, **105**:7052-7057.
26. Anantharaman K, Hausmann B, Jungbluth SP, Kantor RS, Lavy A, Warren LA, Rappe MS, Pester M, Loy A, Thomas BC, Banfield JF: **Expanded diversity of microbial groups that shape the dissimilatory sulfur cycle.** *Isme Journal* 2018, **12**:1715-1728.
27. Tan S, Liu J, Fang Y, Hedlund BP, Lian ZH, Huang LY, Li JT, Huang LN, Li WJ, Jiang HC, et al: **Insights into ecological role of a new deltaproteobacterial order Candidatus Acidulodesulfobacterales by metagenomics and metatranscriptomics.** *Isme Journal* 2019, **13**:2044-2057.
28. Muller AL, Kjeldsen KU, Rattei T, Pester M, Loy A: **Phylogenetic and environmental diversity of DsrAB-type dissimilatory (bi) sulfite reductases.** *ISME Journal* 2015, **9**:1152-1165.
29. Stewart FJ, Dmytrenko O, DeLong EF, Cavanaugh CM: **Metatranscriptomic analysis of sulfur oxidation genes in the endosymbiont of Solemya velum.** *Frontiers in Microbiology* 2011, **2**.
30. Shi L, Dong HL, Reguera G, Beyenal H, Lu AH, Liu J, Yu HQ, Fredrickson JK: **Extracellular electron transfer mechanisms between microorganisms and minerals.** *Nature Reviews Microbiology* 2016, **14**:651-662.
31. Melton ED, Swanner ED, Behrens S, Schmidt C, Kappler A: **The interplay of microbially mediated and abiotic reactions in the biogeochemical Fe cycle.** *Nature Reviews Microbiology* 2014, **12**:797-808.
32. Castelle C, Guiral M, Malarte G, Ledgham F, Leroy G, Brugna M, Giudici-Ortoni MT: **A new iron-oxidizing/O₂-reducing supercomplex spanning both inner and outer membranes, isolated from the extreme acidophile Acidithiobacillus ferrooxidans.** *Journal of Biological Chemistry* 2008, **283**:25803-25811.
33. Barco RA, Emerson D, Sylvan JB, Orcutt BN, Meyers MEJ, Ramirez GA, Zhong JD, Edwards KJ: **New Insight into Microbial Iron Oxidation as Revealed by the Proteomic Profile of an Obligate Iron-Oxidizing Chemolithoautotroph.** *Applied and Environmental Microbiology* 2015, **81**:5927-5937.
34. Garber AI, Nealson KH, Okamoto A, McAllister SM, Chan CRS, Barco RA, Merino N: **FeGenie: A Comprehensive Tool for the Identification of Iron Genes and Iron Gene Neighborhoods in Genome and Metagenome Assemblies.** *Frontiers in Microbiology* 2020, **11**.
35. Liu J, Wang ZM, Belchik SM, Edwards MJ, Liu CX, Kennedy DW, Merkley ED, Lipton MS, Butt JN, Richardson DJ, et al: **Identification and characterization of MtoA: a decaheme c-type cytochrome of**

- the neutrophilic Fe(II)-oxidizing bacterium *Sideroxydans lithotrophicus ES-1*. *Frontiers in Microbiology* 2012, **3**.
36. Lower BH, Shi L, Yongsunthon R, Droubay TC, McCready DE, Lower SK: **Specific bonds between an iron oxide surface and outer membrane cytochromes MtrC and OmcA from *Shewanella oneidensis* MR-1**. *Journal of Bacteriology* 2007, **189**:4944-4952.
 37. Evans PN, Boyd JA, Leu AO, Woodcroft B, Parks DH, Hugenholtz P, Tyson GW: **An evolving view of methane metabolism in the Archaea**. *Nature Reviews Microbiology* 2019, **17**:219-232.
 38. Wang YZ, Wegener G, Hou JL, Wang FP, Xiao X: **Expanding anaerobic alkane metabolism in the domain of Archaea**. *Nature Microbiology* 2019, **4**:595-602.
 39. Borrel G, Adam PS, McKay LJ, Chen LX, Sierra-Garcia IN, Sieber CMK, Letourneur Q, Ghoulane A, Andersen GL, Li WJ, et al: **Wide diversity of methane and short-chain alkane metabolisms in uncultured archaea**. *Nature Microbiology* 2019, **4**:603-613.
 40. Scheller S, Yu H, Chadwick GL, McGlynn SE, Orphan VJ: **Artificial electron acceptors decouple archaeal methane oxidation from sulfate reduction**. *Science* 2016, **351**:703-707.
 41. Timmers PHA, Suarez-Zuluaga DA, van Rossem M, Diender M, Stams AJM, Plugge CM: **Anaerobic oxidation of methane associated with sulfate reduction in a natural freshwater gas source**. *Isme Journal* 2016, **10**:1400-1412.
 42. Beal EJ, House CH, Orphan VJ: **Manganese- and Iron-Dependent Marine Methane Oxidation**. *Science* 2009, **325**:184-187.
 43. Dridi B, Fardeau ML, Ollivier B, Raoult D, Drancourt M: **Methanomassiliicoccus luminyensis gen. nov., sp nov., a methanogenic archaeon isolated from human faeces**. *International Journal of Systematic and Evolutionary Microbiology* 2012, **62**:1902-1907.
 44. Dedysh SN, Panikov NS, Liesack W, Grosskopf R, Zhou JZ, Tiedje JM: **Isolation of acidophilic methane-oxidizing bacteria from northern peat wetlands**. *Science* 1998, **282**:281-284.
 45. Dunfield PF, Yuryev A, Senin P, Smirnova AV, Stott MB, Hou SB, Ly B, Saw JH, Zhou ZM, Ren Y, et al: **Methane oxidation by an extremely acidophilic bacterium of the phylum Verrucomicrobia**. *Nature* 2007, **450**:879-U818.
 46. Tveit AT, Hestnes AG, Robinson SL, Schintlmeister A, Dedysh SN, Jehmlich N, von Bergen M, Herbold C, Wagner M, Richter A, Svenning MM: **Widespread soil bacterium that oxidizes atmospheric methane**. *Proceedings of the National Academy of Sciences of the United States of America* 2019, **116**:8515-8524.
 47. Wu ML, van Alen TA, van Donselaar EG, Strous M, Jetten MSM, van Niftrik L: **Co-localization of particulate methane monooxygenase and cd(1) nitrite reductase in the denitrifying methanotroph 'Candidatus Methyloirabilis oxyfera'**. *Fems Microbiology Letters* 2012, **334**:49-56.
 48. Ho A, Kerckhof FM, Luke C, Reim A, Krause S, Boon N, Bodelier PLE: **Conceptualizing functional traits and ecological characteristics of methane-oxidizing bacteria as life strategies**. *Environmental Microbiology Reports* 2013, **5**:335-345.

49. Beck DAC, Kalyuzhnaya MG, Malfatti S, Tringe SG, del Rio TG, Ivanova N, Lidstrom ME, Chistoserdova L: **A metagenomic insight into freshwater methane-utilizing communities and evidence for cooperation between the Methylococcaceae and the Methylophilaceae.** *Peerj* 2013, **1**.
50. Ackerley DF, Gonzalez CF, Keyhan M, Blake R, Martin A: **Mechanism of chromate reduction by the Escherichia coli protein, NfsA, and the role of different chromate reductases in minimizing oxidative stress during chromate reduction.** *Environmental Microbiology* 2004, **6**:851-860.
51. Miao Y, Liao RH, Zhang XX, Wang Y, Wang Z, Shi P, Liu B, Li AM: **Metagenomic insights into Cr(VI) effect on microbial communities and functional genes of an expanded granular sludge bed reactor treating high-nitrate wastewater.** *Water Research* 2015, **76**:43-52.
52. Robins KJ, Hooks DO, Rehm BHA, Ackerley DF: **Escherichia coli Nema Is an Efficient Chromate Reductase That Can Be Biologically Immobilized to Provide a Cell Free System for Remediation of Hexavalent Chromium.** *Plos One* 2013, **8**.
53. Lovley DR, Phillips EJP: **REDUCTION OF CHROMATE BY DESULFOVIBRIO-VULGARIS AND ITS C(3) CYTOCHROME.** *Applied and Environmental Microbiology* 1994, **60**:726-728.
54. Chardin B, Giudici-Ortoni MT, De Luca G, Guigliarelli B, Bruschi M: **Hydrogenases in sulfate-reducing bacteria function as chromium reductase.** *Applied Microbiology and Biotechnology* 2003, **63**:315-321.
55. Michel C, Brugna M, Aubert C, Bernadac A, Bruschi M: **Enzymatic reduction of chromate: comparative studies using sulfate reducing bacteria - Key role of polyheme cytochromes c and hydrogenases.** *Applied Microbiology and Biotechnology* 2001, **55**:95-100.
56. Das S, Dash HR, Chakraborty J: **Genetic basis and importance of metal resistant genes in bacteria for bioremediation of contaminated environments with toxic metal pollutants.** *Applied Microbiology and Biotechnology* 2016, **100**:2967-2984.
57. Ramirez-Diaz MI, Diaz-Perez C, Vargas E, Riveros-Rosas H, Campos-Garcia J, Cervantes C: **Mechanisms of bacterial resistance to chromium compounds.** *Biometals* 2008, **21**:321-332.
58. Alvarez AH, Moreno-Sanchez R, Cervantes C: **Chromate efflux by means of the ChrA chromate resistance protein from Pseudomonas aeruginosa.** *Journal of Bacteriology* 1999, **181**:7398-7400.
59. Bhatia SK, Yang YH: **Microbial production of volatile fatty acids: current status and future perspectives.** *Reviews in Environmental Science and Bio-Technology* 2017, **16**:327-345.
60. Hattori S: **Syntrophic acetate-oxidizing microbes in methanogenic environments.** *Microbes and Environments* 2008, **23**:118-127.
61. Sieber JR, Sims DR, Han C, Kim E, Lykidis A, Lapidus AL, McDonald E, Rohlin L, Culley DE, Gunsalus R, McInerney MJ: **The genome of Syntrophomonas wolfei: new insights into syntrophic metabolism and biohydrogen production.** *Environmental Microbiology* 2010, **12**:2289-2301.
62. Dombrowski N, Teske AP, Baker BJ: **Expansive microbial metabolic versatility and biodiversity in dynamic Guaymas Basin hydrothermal sediments.** *Nature Communications* 2018, **9**.
63. Hao LP, Michaelsen TY, Singleton CM, Dottorini G, Kirkegaard RH, Albertsen M, Nielsen PH, Dueholm MS: **Novel syntrophic bacteria in full-scale anaerobic digesters revealed by genome-centric**

- metatranscriptomics.** *Isme Journal* 2020, **14**:906-918.
64. Finke N, Vandieken V, Jorgensen BB: **Acetate, lactate, propionate, and isobutyrate as electron donors for iron and sulfate reduction in Arctic marine sediments, Svalbard.** *Fems Microbiology Ecology* 2007, **59**:10-22.
65. Grigoryan AA, Cornish SL, Buziak B, Lin S, Cavallaro A, Arensdorf JJ, Voordouw G: **Competitive oxidation of volatile fatty acids by sulfate- and nitrate-reducing bacteria from an oil field in Argentina.** *Applied and Environmental Microbiology* 2008, **74**:4324-4335.
66. Liu YW, Zhang YB, Ni BJ: **Evaluating Enhanced Sulfate Reduction and Optimized Volatile Fatty Acids (VFA) Composition in Anaerobic Reactor by Fe (III) Addition.** *Environmental Science & Technology* 2015, **49**:2123-2131.
67. Adam PS, Borrel G, Gribaldo S: **Evolutionary history of carbon monoxide dehydrogenase/acetyl-CoA synthase, one of the oldest enzymatic complexes (vol 115, Pg E1166, 2018).** *Proceedings of the National Academy of Sciences of the United States of America* 2018, **115**:E5836-E5837.
68. Karri S, Sierra-Alvarez R, Field JA: **Zero valent iron as an electron-donor for methanogenesis and sulfate reduction in anaerobic sludge.** *Biotechnology and Bioengineering* 2005, **92**:810-819.
69. Kang DWD, Froula J, Egan R, Wang Z: **MetaBAT, an efficient tool for accurately reconstructing single genomes from complex microbial communities.** *Peerj* 2015, **3**.
70. Parks DH, Imelfort M, Skennerton CT, Hugenholtz P, Tyson GW: **CheckM: assessing the quality of microbial genomes recovered from isolates, single cells, and metagenomes.** *Genome Research* 2015, **25**:1043-1055.
71. Chen LX, Mendez-Garcia C, Dombrowski N, Servin-Garciduenas LE, Eloie-Fadrosh EA, Fang BZ, Luo ZH, Tan S, Zhi XY, Hua ZS, et al: **Metabolic versatility of small archaea Micrarchaeota and Parvarchaeota.** *Isme Journal* 2018, **12**:756-775.
72. Chen IMA, Chu K, Palaniappan K, Pillay M, Ratner A, Huang JH, Huntemann M, Varghese N, White JR, Seshadri R, et al: **IMG/M v.5.0: an integrated data management and comparative analysis system for microbial genomes and microbiomes.** *Nucleic Acids Research* 2019, **47**:D666-D677.
73. Wu M, Scott AJ: **Phylogenomic analysis of bacterial and archaeal sequences with AMPHORA2.** *Bioinformatics* 2012, **28**:1033-1034.
74. Hug LA, Baker BJ, Anantharaman K, Brown CT, Probst AJ, Castelle CJ, Butterfield CN, Hensdorf AW, Amano Y, Ise K, et al: **A new view of the tree of life.** *Nature Microbiology* 2016, **1**.
75. Katoh K, Asimenos G, Toh H: **Multiple Alignment of DNA Sequences with MAFFT.** In *Bioinformatics for DNA Sequence Analysis. Volume 537.* Edited by Posada D; 2009: 39-64: *Methods in Molecular Biology*].
76. Capella-Gutierrez S, Silla-Martinez JM, Gabaldon T: **trimAl: a tool for automated alignment trimming in large-scale phylogenetic analyses.** *Bioinformatics* 2009, **25**:1972-1973.
77. Nguyen LT, Schmidt HA, von Haeseler A, Minh BQ: **IQ-TREE: A Fast and Effective Stochastic Algorithm for Estimating Maximum-Likelihood Phylogenies.** *Molecular Biology and Evolution* 2015, **32**:268-274.

Figures

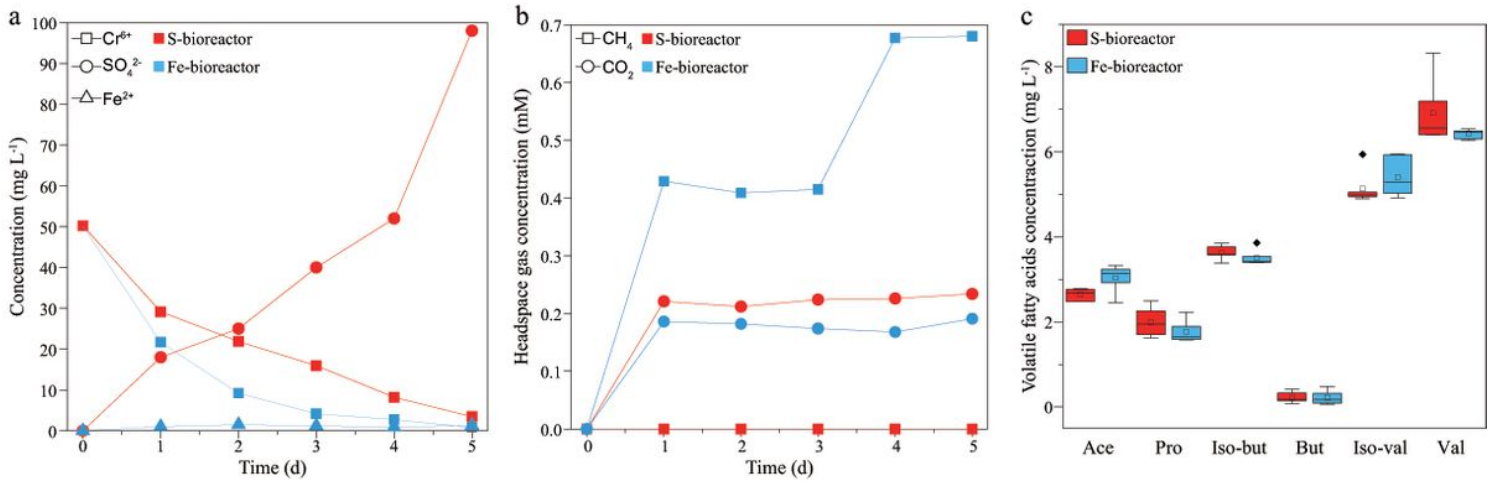


Figure 1

The kinetic of intermediates in one cycle (5 days) of the S- and -Fe bioreactors. (a) Cr⁶⁺, SO₄²⁻, and Fe²⁺; (b) CH₄ and CO₂; (c) acetate (Ace), propionic acid (Pro), isobutyric acid (Iso-but), butyric acid (But), isovaleric acid (Iso-val), and valeric acid (Val). The red color represents the S-bioreactor and the blue color represents the Fe-bioreactor.

a

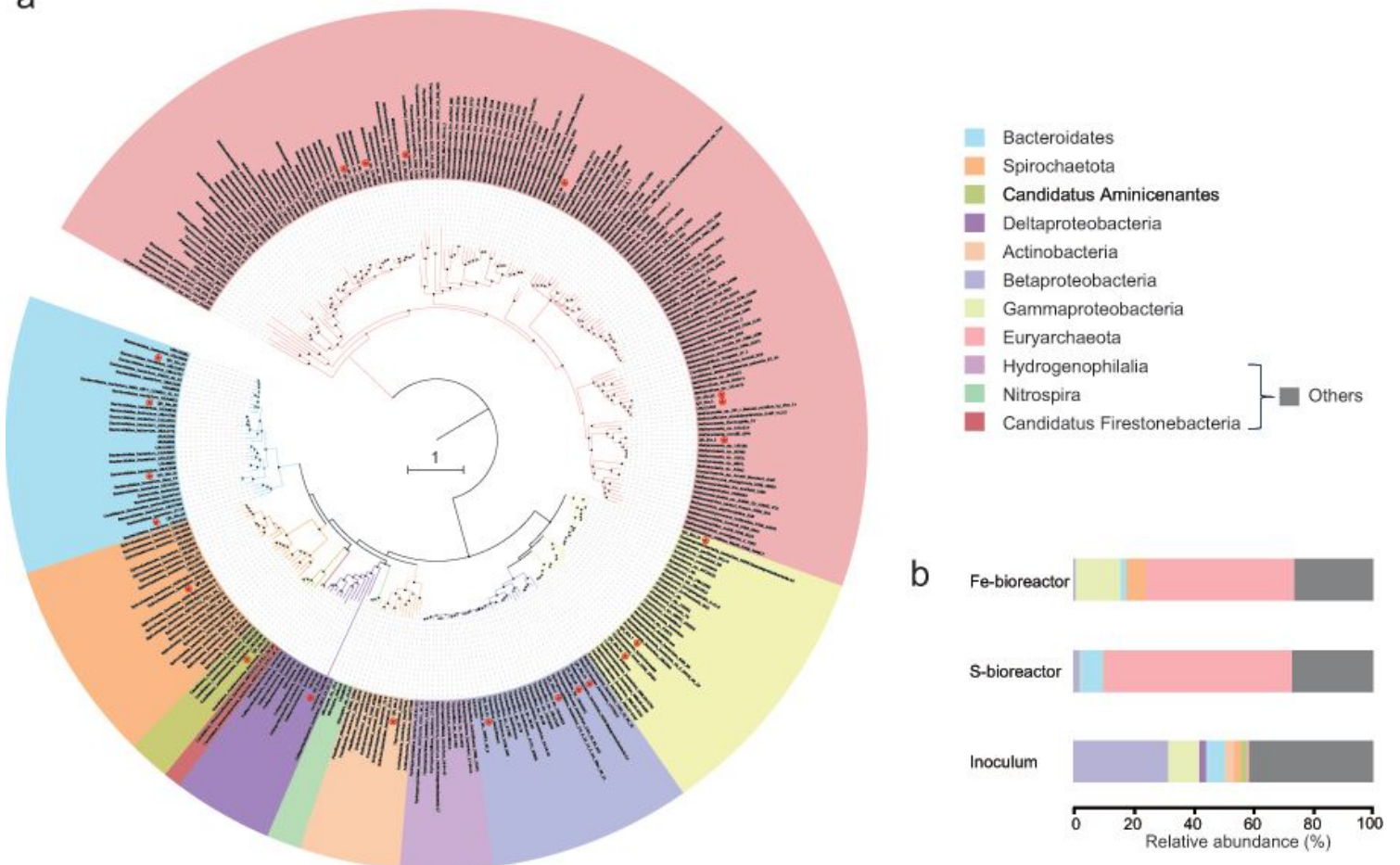


Figure 2

Phylogenetic placement of the 23 assembled bins. (a) The maximum-likelihood phylogenetic tree was constructed using the concatenated alignment of 16 ribosomal proteins. Bootstrap values were based on 100 replicates, and percentages $\geq 75\%$ are shown with black circles. (b) Taxonomy composition (phylum or class level) in S-bioreactor, Fe-bioreactor, and inoculum based on the phylogenetic placement and relative abundance of each bin.

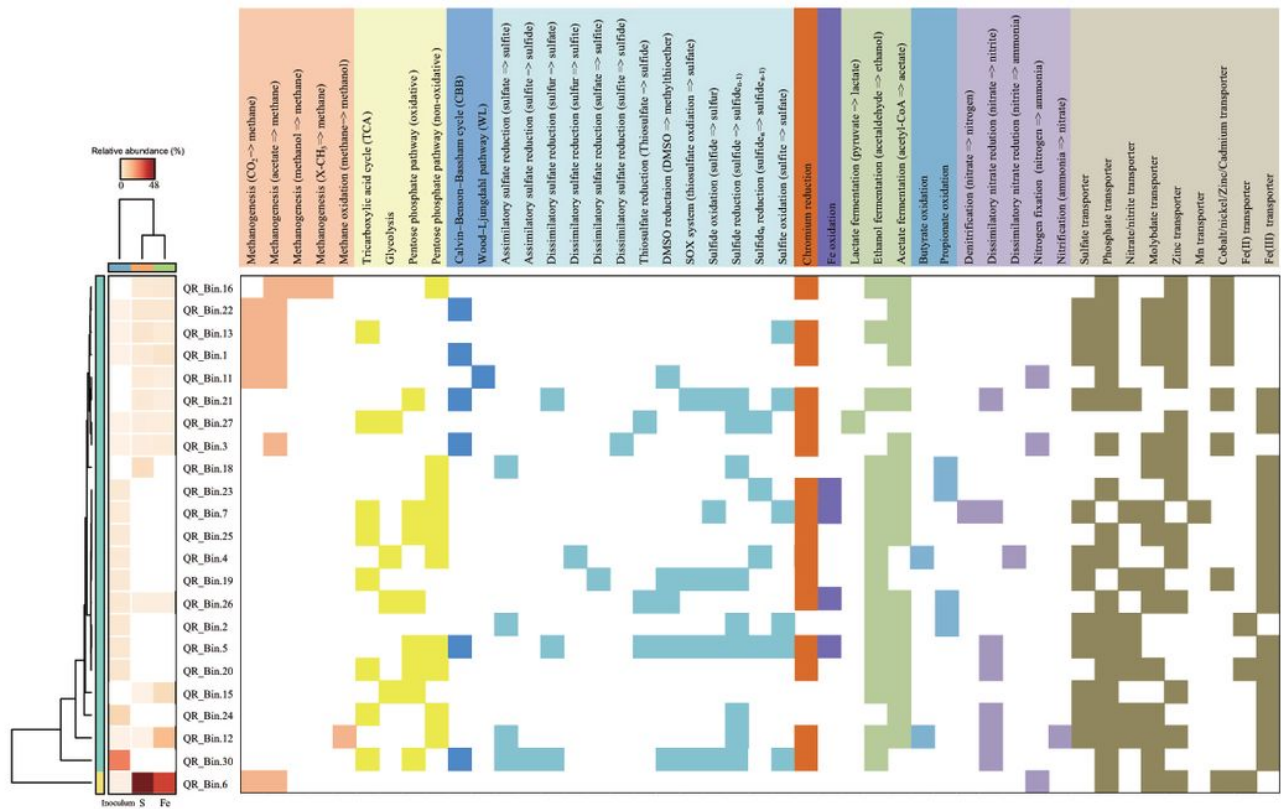


Figure 3

Presence of core metabolic genes involved in methane, carbon fixation, sulfur, iron, chromium, fermentation, nitrogen metabolisms in each bin in the S-bioreactor, Fe-bioreactor, and inoculum. The relative abundance (%) of each bin was calculated by dividing the coverage of its rpS3 by the total coverage of all rpS3 in the community.

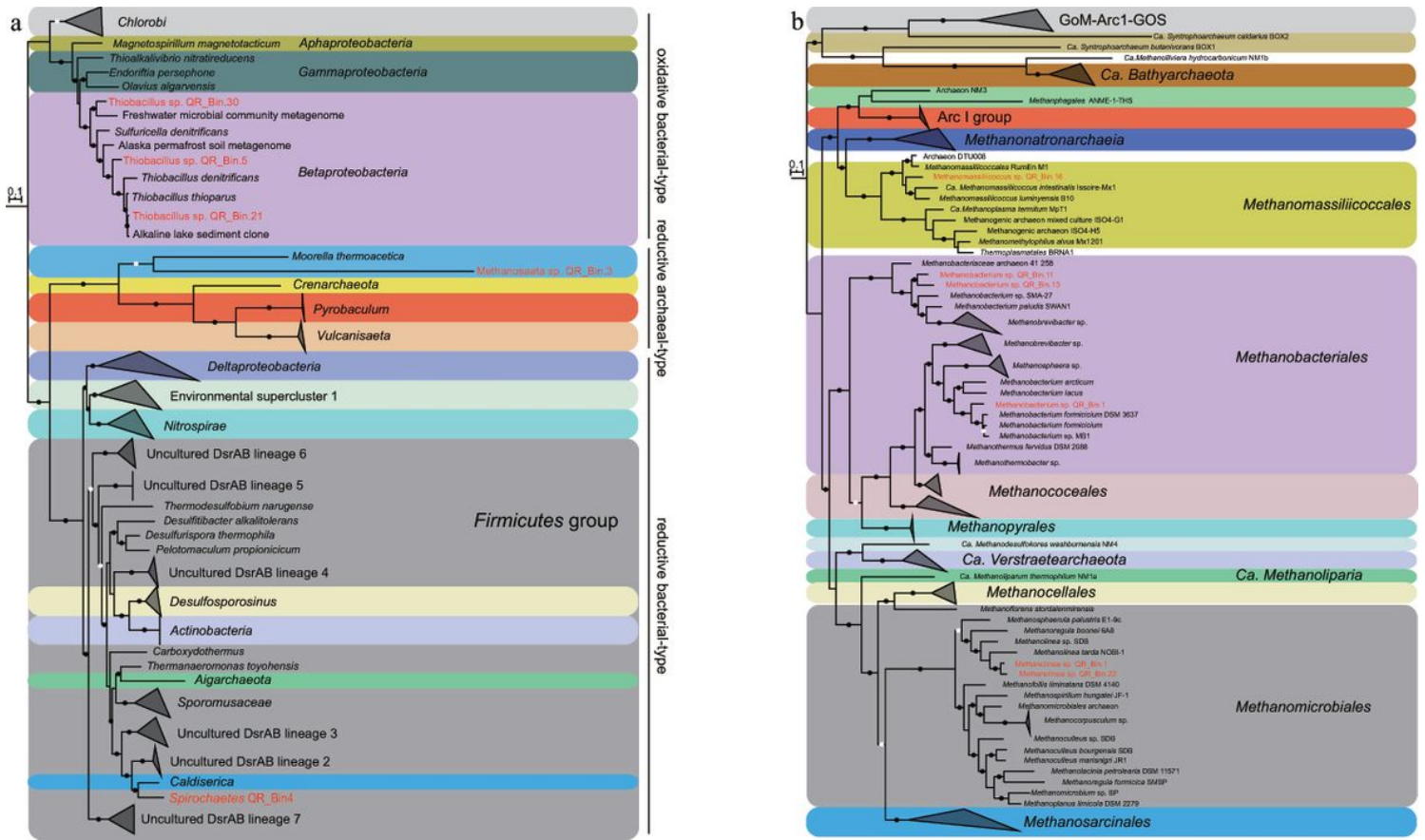


Figure 4

Phylogenetic analysis of the concatenated DsrAB (a) and McrABG (b) proteins. The assembled bins were marked as red color. Bootstrap values were based on 100 replicates, and only bootstrap values higher than 75% are shown with black circles.

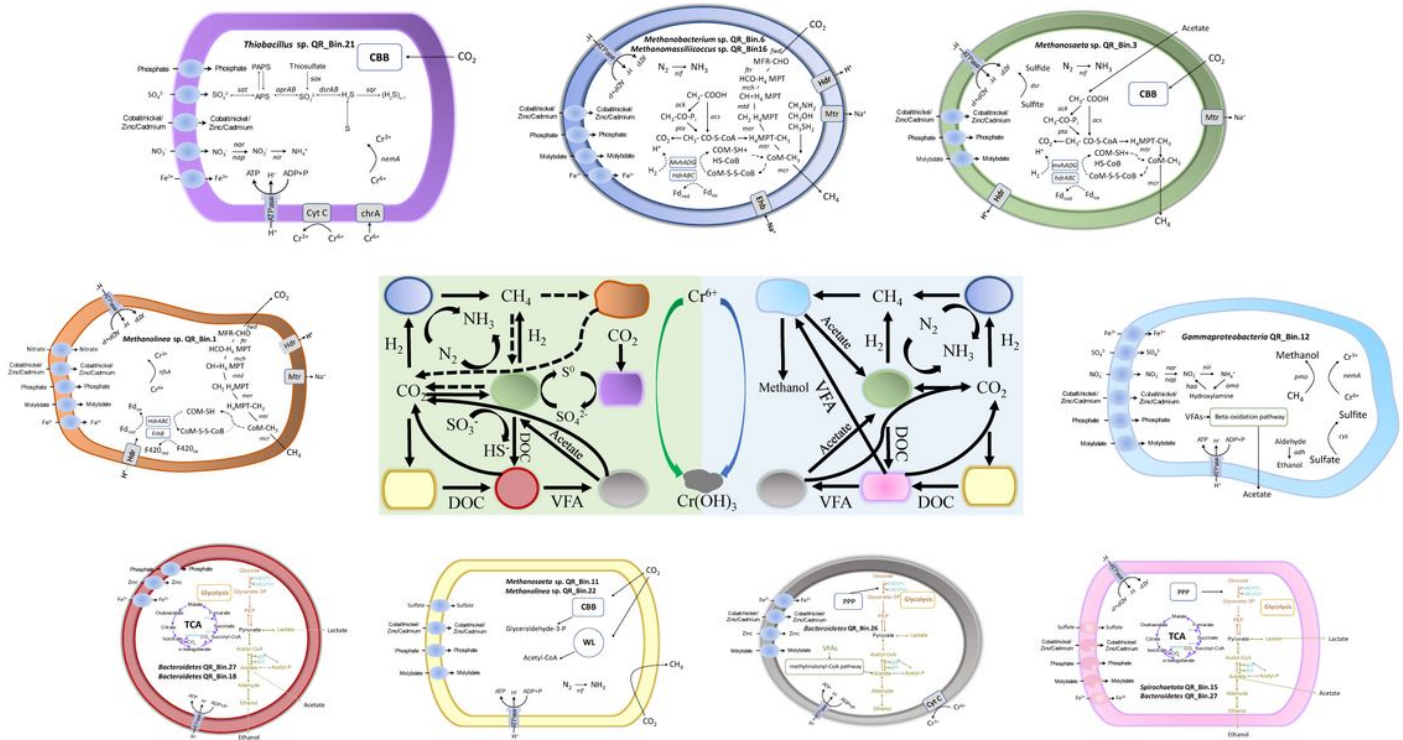


Figure 5

Cooperation and interaction model for representative genomes assembled from metagenomic data of the communities in S-bioreactor (green shading) and Fe-bioreactor (blue shading).

Supplementary Files

This is a list of supplementary files associated with this preprint. Click to download.

- [SupplementaryTableS1.xlsx](#)
- [Supplementaryfigures.docx](#)
- [SupplementaryTableS2.xlsx](#)
- [SupplementaryTableS3.xlsx](#)
- [SupplementaryTableS4.xlsx](#)